ARTICLE
Journal of Cellular Biochemistry 111:350–361 (2010)

Journal of Cellular Biochemistry

Bone Matrix Proteins and Extracellular Acidification: Potential Co-Regulators of Osteoclast Morphology

Azza Gramoun,[1] Tetsuya Goto,[2] Tommy Nordström,[3] Ori D. Rotstein,[4] Sergio Grinstein,[5] Johan N.M. Heersche,[1] and Morris F. Manolson[1*]

[1]*Faculty of Dentistry, University of Toronto, Toronto, ON, Canada*
[2]*Division of Anatomy, Kyushu Dental College, Kitakyushu, Japan*
[3]*Institute of Biomedicine and Physiology, University of Helsinki, Helsinki, Finland*
[4]*Department of Surgery, St Michael's Hospital and University of Toronto, ON, Canada*
[5]*Division of Cell Biology, The Hospital for Sick Children, Toronto, ON, Canada*

ABSTRACT

Osteoclasts are signaled by the bone matrix proteins fibronectin (FN), vitronectin (VN), and osteopontin (OPN) via integrins. To perform their resorptive function, osteoclasts cycle between compact (polarized), spread (non-resorbing) and migratory morphologies. Here we investigate the effects of matrix proteins on osteoclast morphology and how those effects are mediated using RAW 264.7 cells differentiated into osteoclasts on FN, VN, and OPN-coated culture dishes. After 96 h, 80% of osteoclasts on FN were compact while 25% and 16% on VN were in compact and migratory states respectively. In contrast, OPN induced osteoclast spreading. Furthermore, osteoclasts formed on VN and FN were two- to fourfold smaller than those formed on OPN in the 21–30 nuclei/osteoclast group. These effects were not due to defects in cytoskeletal reorganization of osteoclasts on VN and FN, demonstrated by the ability of these cells to spread in response to 35 ng/ml macrophage colony stimulating factor (M-CSF). Conversely, osteoclasts on OPN failed to spread when induced by M-CSF. Moreover, the extracellular pH on FN and VN (7.25 and 7.3, respectively) was significantly lower than that on OPN (~7.4). We further investigated the role of extracellular pH and found that at pH 7.5 the duration of an osteoclast's compact phase was 25.6 min and that of the spread phase was 62.5 min. Reducing the pH to 7.0 increased the frequency of osteoclast cycling by threefold. These results show that matrix proteins play a role in regulating osteoclast morphology, possibly via altering extracellular and intracellular pH. J. Cell. Biochem. 111: 350–361, 2010.

KEY WORDS: OSTEOCLAST; MATRIX PROTEINS; PH; BONE; FIBRONECTIN

Bone resorption is an essential process required for maintenance of bone integrity. Osteoclasts, the cells exclusively responsible for bone resorption, are of myeloid lineage and form by fusion of mononucleated precursors. Osteoclasts are dynamic and versatile cells. During their functional cycle, osteoclasts alternate between migration and resorption and occasionally resting phases [Owens and Chambers, 1993].

The focus of this study revolves around determining factors affecting osteoclast morphology; thus, we will first review relevant aspects of osteoclast morphology. During an osteoclast functional cycle leading to resorption, the cell undergoes a series of actin cytoskeletal rearrangements resulting in different morphologies. More specifically, an osteoclast was shown to exist in one of three phenotypes; spread (flat), migratory (motile), and polarized (compact).

A migrating osteoclast is characterized by its dynamic membrane rufflings and lamellipodial formation at the leading edge. During migration podosomes, the osteoclast attachment complexes are disrupted at the trailing edge; allowing for a forward sliding motion of the cell [Pilkington et al., 2001; Chellaiah and Hruska, 2003].

A resorbing osteoclast is polarized baso-apically creating three functional membrane domains facilitating resorption; the ruffled border, the functional secretory domain and the baso-lateral domain. The ruffled border is juxtaposed to the bone surface and is enclosed in a junctional structure known as the sealing zone. Active membrane trafficking occurs at the ruffled border sequestering proton pumps, chloride channels and vesicles containing proteases to the area. The sealing zone is a dense F-actin band surrounded by two narrow vinculin rings on both its sides [Lakkakorpi and Vaananen, 1991; Jurdic et al., 2006]. It surrounds

Grant sponsor: Canadian Institutes of Health Research (CIHR); Grant number: FRN MOP-79322.
*Correspondence to: Dr. Morris F. Manolson, Faculty of Dentistry, University of Toronto, 124 Edward Street, Toronto, ON Canada M5G 1G6. E-mail: m.manolson@utoronto.ca
Received 17 December 2009; Accepted 17 May 2010 • DOI 10.1002/jcb.22705 • © 2010 Wiley-Liss, Inc.
Published online 19 May 2010 in Wiley Online Library (wileyonlinelibrary.com).

the ruffled border and delineates a tightly sealed acidic compartment between the ruffled border and the bone surface. Finally, a spread osteoclast is a flat, non-resorbing cell, that does not exhibit an actin ring, and is neither migrating nor resorbing. This phase can sometimes be seen between two functional cycles.

These alternating events of the resorption cycle occur continuously on bone and require rapid cycles of actin polymerization and depolymerization. Similar phases can also be seen in osteoclasts on tissue culture polystyrene (TCP) and glass, with the exception of the ability of osteoclasts to form a sealing zone which is substrate dependent and is governed entirely by the mineral content of the substrate [Saltel et al., 2004]. While a sealing zone is seen exclusively in osteoclasts on a resorbable surface, another actin rich podosome super-structure known as the podosome belt is located paramarginally in a mature osteoclast on glass and TCP [Akisaka et al., 2001]. Even though the two structures are similar, they are distinctive in their actin organization [Geblinger et al., 2009]. A podosome belt is made of an F-actin condensation known as a podosome core, surrounded by branches of finely interconnected fibers called the actin cloud [Luxenburg et al., 2007]. Nonetheless, osteoclasts with podosome belts are still capable of degrading matrix proteins coated on TCP [Badowski et al., 2008; Desai et al., 2008].

The extracellular matrix proteins (ECM) are a large family of macromolecules that contribute to the bio-mechanical properties of bone. Among the more abundant bone matrix proteins are fibronectin (FN), vitronectin (VN), and osteopontin (OPN), all three of which are Arg-Gly-Asp (RGD) containing glycoproteins. The RGD driven attachment of osteoclasts to those proteins occurs via surface receptors known as integrins. Cell binding to these ECM proteins is the basis of cell attachment and survival. Cell spreading is also affected by integrin mediated attachment and therefore this process can also dictate cell shape.

Despite the abundance of ECM proteins within bone, few studies have focused on their effects on osteoclast shape and morphology. Early studies have found that the proportion of compact osteoclasts is greater when mature rat osteoclasts are plated on dentine or type I collagen compared to glass [Arkett et al., 1992]. Saltel et al. [2004] have shown that a mineralized matrix is required for the formation of a sealing zone when mature osteoclasts are seeded on a substrate. Additionally, an organic matrix, such as collagen I, was not sufficient for sealing zone formation but allowed for the formation of podosome belts. Various aspects of osteoclast attachment to different bone matrix proteins have been explored [Flores et al., 1992; Hu et al., 2008] but there has not yet been any studies on how the matrix affects the morphology during osteoclastogenesis.

Electrochemical balance and pH homeostasis are crucial for cell survival. pH regulation is not only essential for osteoclast survival but is also pivotal to optimal resorptive capacity. V-ATPases, HCO_3^-/Cl^- exchangers, Na^+/H^+ antiporters, p62/CLIC-5b, ClC-7, and carbonic anhydrase II have all been shown to play an important role in osteoclast pH regulation and resorption [Hall and Chambers, 1990; Asotra et al., 1994; Nordström et al., 1995; Bastani et al., 1996; Gupta et al., 1996; Schlesinger et al., 1997; Kornak et al., 2001; Manolson et al., 2003; Edwards et al., 2006]. Evidence indicates that extracellular acidification affects pH*i* regulation and osteoclast morphology [Nordström et al., 1997].

Here we have investigated for the first time the morphological effects of the matrix proteins FN, VN, and OPN on differentiating osteoclasts and the role of extracellular pH as a regulator of osteoclast shape. Our results suggest a relationship between matrix proteins and extracellular pH and raise the possibility that they are co-regulators of osteoclast morphology.

MATERIALS AND METHODS

MATERIALS

Human FN was purchased from Sigma–Aldrich Ltd. (St. Louis, MO) and human VN was purchased from BD Biosciences (BD Labwares, Franklin Lakes, NJ). Bovine OPN was kindly provided by the late Dr. J. Sodek (University of Toronto). Recombinant mouse macrophage colony stimulating factor (M-CSF) was obtained from Calbiochem (EMD BioSciences, Inc., San Diego, CA). The RAW 264.7 cell line was obtained from American Type Culture Collection (ATCC, Manassas, VA). 4-[2-hydroxyethyl] piperazine-*N*′-[ethanesulfonic acid] (HEPES), amiloride, 4,4′-diisothiocyanatostilbene-2,2′-disulfonic acid (DIDS), and acetazolamide were obtained from Sigma–Aldrich Ltd. Dulbecco's modified Eagle's medium (DMEM) and α-Minimum essential medium (α-MEM) without bicarbonate containing 25 mM HEPES, antibiotics and antimycotics (penicillin/streptomycin, fungizone) and fetal bovine serum (FBS) were obtained from Invitrogen (Carlsbad, CA). Fast red violet LB salt and naphthol AS-MX, were obtained from Sigma–Aldrich Ltd. Six- and 12-well plastic Falcon™ tissue culture plates were purchased from BD Biosciences (BD Labwares, Franklin Lakes, NJ). 2′,7′-bis-(2-Carboxyethyl)-5 (6)-carboxyfluorescein, acetoxymethyl ester (BCECF, AM) was bought from Molecular Probes Inc. (Eugene, OR). Bafilomycin A_1 was bought from Kamiya Biomedical Co. (Thousand Oaks, CA).

RAW 264.7-DERIVED OSTEOCLAST CULTURES

Twelve-well tissue culture polystyrene (TCP) plates were pre-coated with 350 μl of 10 μg/ml of FN, VN, or OPN dissolved in phosphate buffered saline (PBS) over night (O/N) at 4°C. To increase the amount of proteins physically adsorbed on to the TCP plates, the matrix proteins were incubated for an additional 1 h at 37°C. After the aspiration of the matrix proteins, the wells were subsequently blocked using 1% BSA in PBS for 1 h at 37°C in a CO_2 incubator to minimize nonspecific binding of serum proteins to TCP. Finally the wells were washed 3× with 100 μl PBS and left in PBS until cells were plated to prevent denaturing of the proteins. BCA protein assay was used to assess the amount of protein adsorbed to TCP.

RAW264.7 (RAW) cells were plated on the ECM coated wells and cultured in DMEM supplemented with 10% FBS, 100 μg/ml penicillin/streptomycin and 0.2 μg/ml fungizone and incubated at 37°C in 5% CO_2. Osteoclasts were generated using 75 ng/ml receptor activator of NFκB ligand (RANKL). After 96 h of incubation, multinucleated osteoclasts were observed. When cultures were stopped using 4% formaldehyde for 5–6 min, these cells stained positive for tartrate resistant acid phosphatase activity (TRAP). Cell morphology and number were determined using bright field microscopy. The number of osteoclasts with compact, migratory and spread morphologies were count on each of the adsorbed ECM

proteins and were plotted as a percentage of the total number of osteoclasts with >3 nuclei. No specific morphologies could be identified in osteoclasts with 2 and 3 nuclei.

Osteoclast spreading on ECM proteins was assessed at 96 h after their incubation with M-CSF. This was achieved by washing cultures 3× with cold PBS–Ca–Mg. The cells were then incubated with PBS–Ca–Mg for 45 min at 37°C and 5% CO_2. The cultures were subsequently incubated for 2.5 h in media without FBS and with or without 35 ng/ml M-CSF. The cultures were then fixed and stained for TRAP activity.

RABBIT OSTEOCLAST ISOLATION

Animal protocols were approved by the Animal Care Committees at the University of Toronto. Osteoclasts were isolated from the long bones of newly born New Zealand rabbits, as described previously [Kanehisa and Heersche, 1988; Gramoun et al., 2007]. Briefly, bones were cleaned and minced mechanically in 100 mm glass Petri dishes containing 10 ml of α-MEM supplemented with 10% FBS and 1% penicillin/streptomycin. Bone fragments were transferred into 50 ml Falcon tubes and cells were resuspended by repeated passage (30 times) through a wide-bore Pasteur pipette. The bone fragments were allowed to briefly settle and the cell suspension was transferred to another tube. An additional 6 ml of supplemented media was then added to the remaining minced bones in the Petri dish and the previous steps were repeated. Aliquots (100 μl) of cell suspension were plated in 6-well TCP plates. Osteoclasts were allowed to attach for 1 h (37°C, 5% CO_2), after which 1.5 ml of supplemented medium was added. After a further 18-h period, the cultures were washed gently with α-MEM using a widebore Pasteur pipette to remove non-attached cells. This technique of cell isolation generates a mixed culture of attached osteoclasts, prefusion osteoclasts, and stromal cells. Only multinucleated cells identified under phase contrast were monitored for morphological changes.

TARTRATE-RESISTANT ACID PHOSPHATASE (TRAP) STAINING

TRAP staining was carried out according to the protocol described in BD Biosciences Technical Bulletin #445. Briefly, cell cultures were washed 3× with PBS, fixed with 4% formaldehyde for 5–6 min and incubated in TRAP staining solution (50 mM acetate buffer, 30 mM sodium tartrate, 0.1 mg/ml Naphtol AS-MX phosphate, 0.1% (w/v) Triton X-100, and 0.3 mg/ml Fast Red Violet LB stain) for 10 min until the desired staining intensity was reached. The TRAP staining solution was aspirated and the cells were washed 3× with dH2O.

ASSESSMENT OF OSTEOCLAST MORPHOLOGICAL CHANGES USING TIME-LAPSE MICROSCOPY

After an 18-h incubation period of rabbit osteoclasts from the time of their isolation, the cultures were washed gently with bicarbonate free α-MEM supplemented media containing 25 mM HEPES, using a widebore Pasteur pipette to remove non-attached cells. The cultures were subsequently incubated with 1.5 ml α-MEM supplemented media containing 25 mM HEPES, with the pH adjusted to pH 7.0 or 7.5 for up to 24 h. Media pH was adjusted using 0.5 M solution of either hydrochloric acid or sodium hydroxide.

TCP plates were placed in the incubation chamber of a Nikon Diaphot phase-contrast inverted microscope for time-lapse photography using a SONY AVC D5 camera. Some plates were initially incubated at pH 7.5 for 5–6 h, then washed once and the medium was changed to a fresh medium of pH 7.0.

To determine the role of V-ATPases, Na^+/H^+ antiporters, anion exchangers and carbonic anhydrase in regulating changes in osteoclast morphology, osteoclasts were incubated with medium at pH 7.0 for 3 h after which the different inhibitors were added. We tested the effects of 100 nM bafilomycin A1 (V-ATPase inhibitor); 1 mM amiloride (Na^+/H^+ antiporter inhibitor); 100 μM DIDS (anion exchanger inhibitor), and 10 μM acetazolamide (carbonic anhydrase inhibitor) by incubating the cells with each of these inhibitors for 3 h at pH 7.0.

MORPHOMETRICAL ANALYSIS OF CHANGES IN OSTEOCLAST'S MORPHOLOGY

Using a Leica DMIRE2 microscope, micrographs of cultures on different ECM proteins were acquired after the cells were fixed and TRAP stained. The perimeter of TRAP+ osteoclasts was outlined manually and the area was measured using Openlab® imaging system. Osteoclasts were divided into groups based on their size determined by the number of nuclei/osteoclast.

Morphometrical analysis of rabbit osteoclast spreading and motility were performed using the method described by Zaidi et al. [1992]. The spread area, A(t) at each time t was obtained by tracing the cell perimeter and its area was quantified using Zeiss Zidas system. Area was expressed as a percentage of mean area ⟨A0⟩ of the osteoclast at the start of the experiment, resulting in the "area descriptor", A(t)/A0 (cell spreading). Motility was evaluated by overlaying the traces outlines obtained at time t on previous outline at time $(t - \Delta t)$, $\Delta t = 10$ min in the experiment. The degree of cell retraction, [Δr], was defined as the area falling within the area $[A(t - \Delta t)]$, but not [A(t)]. Conversely, cell spreading or protrusion, [Δp], was defined by the set of pixels falling within [A(t)] but not $[A(t - \Delta t)]$. This resulted in the "motility descriptor" $([\Delta r] + [\Delta p])/A(t)$.

SCANNING ELECTRON MICROSCOPY

Cultured cells were washed twice with medium and fixed with 2.5% glutaraldehyde and 3.7% paraformaldehyde in 0.1 M PBS for 2 h. After fixation, the specimens were rinsed with PBS, dehydrated through a graded ethanol series and critical-point dried after ethanol was substituted with CO_2. The specimens were places on an aluminum slab, coated with gold sputter and observed using Hitachi S-2500 operated in the secondary electron mode at 10 kV.

INTRACELLULAR pH MEASUREMENTS

As described previously, rabbit osteoclasts were isolated and incubated with 1.5 ml α-MEM supplemented media containing 25 mM HEPES, with the pH adjusted to pH 7.0 or 7.5 for up to 24 h prior to measuring the cytoplasmic pH. Media pH was adjusted using 0.5 M solution of either hydrochloric acid or sodium hydroxide. For microfluorimetric studies, osteoclasts were analyzed essentially as described by [Nordström et al., 1995]. Briefly, the cells were plated for 48 h on acid washed glass coverslips and placed into a Leiden Cover Slip Dish and maintained at 37°C. They were then loaded with BCECF by incubation with 1 μM of the parent acetoxymethyl ester

for 15 min at 37°C. The osteoclasts were next washed with α-MEM and incubated in the indicated conditions. Single cell fluorescence was monitored using a Nikon TMD-Diaphot microscope attached to an M Series Dual Wavelength Illumination System from Photon Technologies Inc. Illumination was shuttered on and off for 2 and 20 s, respectively and the photometric data was recorded at a rate of 5 points/s. Mean values for each 2 s illumination period were plotted against time. Calibration of the fluorescence ratio versus pH was performed using the K^+/H^+ ionophore nigericin. Cells were equilibrated in K^+ medium (140 mM) of varying pH in the presence of 5 μM nigericin and calibration curves were constructed by plotting the extracellular pH (which is assumed to be identical to the internal pH) [Thomas et al., 1979] against the corresponding fluorescence ratio. The resulting curve was sigmoidal with an inflection point = 7.0 as expected from the reported pK_a of BCECF.

STATISTICS

Statistical evaluation was carried out using SPSS 12.0 for Windows using one way analysis of variance (ANOVA) and Dunnett's T3 test. *P*-values less than 0.05 were considered statistically significant.

RESULTS

OSTEOCLASTS FORMED ON FN, VN, AND OPN HAVE DISTINCT MORPHOLOGIES AND PLANAR AREA

To ask whether differentiating osteoclasts in the presence of a specific matrix protein has an effect on their morphology, RAW cells were cultured for 96 h on TCP coated with physically adsorbed 10 μg/ml FN, VN, and OPN. The cultures were subsequently fixed and stained for TRAP activity and the morphology of the cells was assessed. We observed that osteoclasts formed on each of the different ECM proteins had a distinctive and unique morphology. Osteoclasts formed on FN had a "rounded up" or "compact" morphology similar to that seen when osteoclasts are polarized on a resorbable matrix (Fig. 1A). In contrast, osteoclasts on OPN were noticeably more "spread" or "flat" (Fig. 1C). Osteoclasts on VN exhibited either a compact morphology with a condensed cytoplasm similar to that seen on FN or a "motile" or "migrating" morphology (Fig. 1B). Migrating osteoclasts are characterized by having a "leading edge" and a "trailing edge" with ruffling in their lamellipodia. Based on these observations we identified three morphologies (Fig. 1D: compact, migratory and spread) which were

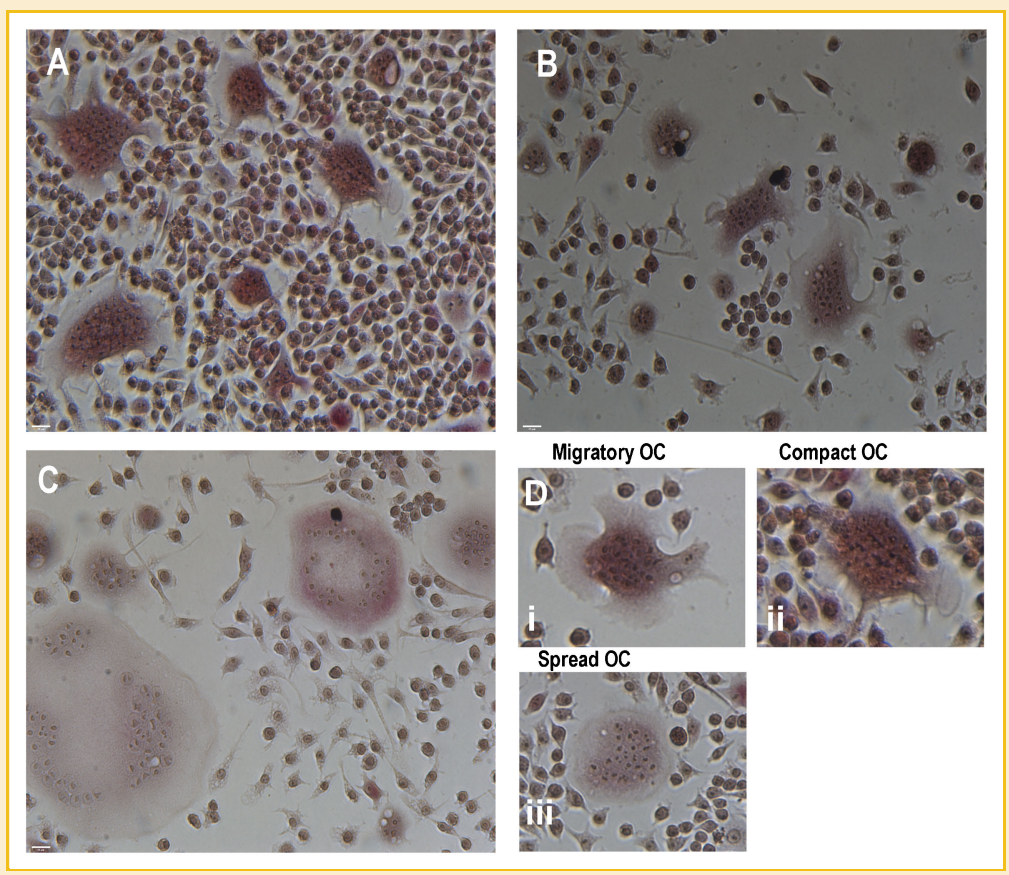

Fig. 1. Osteoclasts differentiated on FN, VN, and OPN have different morphologies. RAW cells were plated on TCP dishes precoated with FN, VN, and OPN at 10 μg/ml. RAW cells were differentiated into osteoclasts for 96 h in the presence of 75 ng/ml RANKL. The cultures were fixed and stained for TRAP activity. Micrographs of osteoclasts cultures on FN (A), VN (B), and OPN (C) were taken using Openlab® Imaging system. Scale bar is 25 μm. Panel D is composed of images of osteoclasts representing the three morphologies that were identified in cultures on FN, VN, and OPN: (i) migratory osteoclast, (ii) compact osteoclast, and (iii) spread osteoclast. Similar results were obtained in three separate experiments.

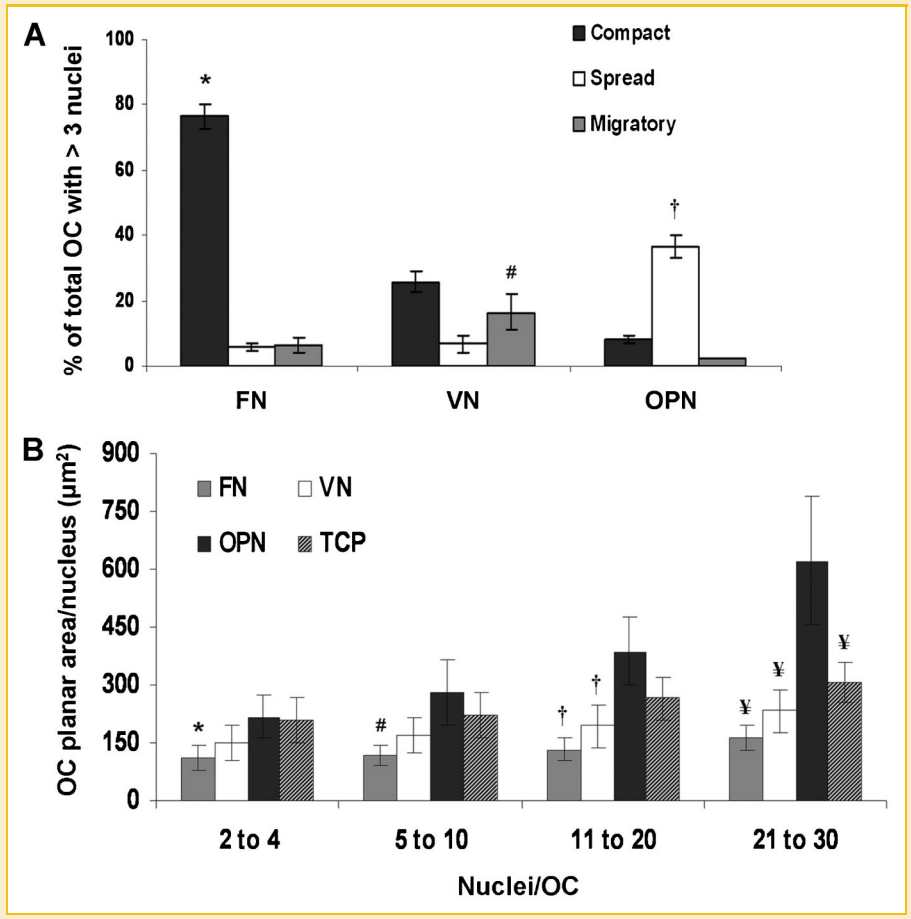

Fig. 2. Osteoclast morphology and planar area are modulated by the ECM proteins FN, VN, and OPN. RAW cells were plated on TCP dishes precoated with FN, VN, and OPN at 10 µg/ml. RAW cells were differentiated into osteoclasts for 96 h in the presence of 75 ng/ml RANKL. The cultures were fixed and stained for TRAP activity and the total number of TRAP+ osteoclasts was counted. Subsequently the number of osteoclasts with a condensed cytoplasm (compact), membrane ruffling (migratory) or flat (spread) morphology was determined and finally the they were plotted as a percentage of osteoclasts with >3 nuclei (A). Each data point represents the pooled results from four dishes per treatment and is expressed per well (means ± SD). $^{*}P$ value <0.05 versus VN and OPN groups, $^{\#}P$ value <0.05 versus FN and OPN groups and $^{\dagger}P$ value <0.05 versus FN and VN groups. Osteoclast perimeter was traced manually and the planar area was measured using Openlab® imaging system. Planar areas measurements were normalized to the number of nuclei/osteoclast and the data was divided into groups based on osteoclast size as defined by its number of nuclei/osteoclast. Each data point represents pooled results from a minimum of 40 osteoclasts per treatment group (means ± SD). $^{*}P$ value <0.05 versus OPN in (2–4) nuclei/osteoclast category, $^{\#}P$ value <0.05 versus OPN in (5–10) nuclei/osteoclast category, † P value <0.05 versus OPN in (11–20) nuclei/osteoclast category and $^{¥}P$ value <0.05 versus OPN in (21–30) nuclei/osteoclast category. Similar results were obtained in three separate experiments. OC = osteoclast.

the prevalent osteoclast morphologies in the cultures. Interestingly, the effects of the ECM proteins on osteoclast morphology were seen only when these proteins were physically adsorbed to TCP but not when they were added in a soluble form.

To quantify this observation, the percentage of osteoclasts conforming to the predetermined morphology criteria was determined and is shown in Figure 2A. Only osteoclasts where one of the three morphologies could clearly be identified were counted and small osteoclasts (≤3 nuclei) were not included as it was difficult to categorize them under any of the three preset morphologies.

On FN, 80% of the total number of osteoclasts was compact, with less than 7% of osteoclasts spread or migratory. Osteoclasts on VN were found to be 25% compact, 7% spread and 16% migratory. Finally, 36% of the total osteoclasts formed on OPN were spread versus 8% and 2% compact and migratory respectively (Fig. 2A). These results show that FN increases the percentage of compact osteoclasts compared to VN and OPN while osteoclasts on OPN were more spread compared to those on FN and VN. The highest percentage of migratory osteoclasts was seen on VN. It is worth noting that while the ECM proteins FN and VN decreased the number of osteoclast formed by ~ 65%, OPN promoted osteoclast formation. Although the ECM proteins modulated osteoclast formation, none of these proteins affected RAW cell viability [Gramoun et al., in preparation].

To further quantify differences in morphology, we measured osteoclast planar area and normalized it to the number of nuclei (Fig. 2B). Osteoclast planar area/nucleus was further divided into four groups based on the number of nuclei to determine if there were differences in area/nucleus ratio among the various osteoclast populations. As compact osteoclasts have smaller planar area than spread osteoclasts, we expected and indeed found that osteoclasts on

FN that had the highest percentage of compact osteoclasts also had a consistently smaller planar area than those on OPN (Fig. 2B), irrespective of osteoclast size (defined by number of nuclei/osteoclasts). By presenting the planar area measurements in 4 groups of osteoclast size (nuclei/osteoclast), one can also see that the ratio of osteoclast planar area per nucleus changed dramatically for osteoclasts on OPN within the 21–30 nuclei group (Fig. 2B). In contrast, the ratio of planar area remained unchanged between all four size groups for TCP, FN, and VN.

M-CSF INDUCES OSTEOCLAST SPREADING ON FN BUT NOT ON OPN

Next, we hypothesized that the differences seen in osteoclast morphology and area on the ECM proteins underlie a defect in the activation of the osteoclast machinery responsible for osteoclast spreading. As M-CSF activates cytoskeletal reorganization leading to osteoclast spreading on TCP, we asked whether osteoclasts on FN, VN, and OPN respond differentially to M-CSF. Osteoclasts differentiated for 96 h on physically adsorbed matrix proteins were induced to retract using cold PBS–Ca–Mg. When cellular retraction was observed, they were subsequently triggered to spread using 35 ng/ml M-CSF.

We observed that the degree of osteoclast spreading changed with osteoclast size. Therefore, to facilitate comparison between the different matrix proteins and eliminate differences originating from osteoclast size, the results were grouped by nuclei per osteoclast. Osteoclasts with more than 30 nuclei did not respond to M-CSF irrespective of matrix, (data not shown) and were excluded. The biggest response to M-CSF on FN, VN, and TCP substrates was seen in osteoclasts containing 11–20 nuclei. The same results were seen in osteoclasts with 21–29 nuclei (data not shown).

Osteoclasts on FN spread appropriately in response to M-CSF, suggesting that the compact shape of the osteoclasts does not arise from a defect in cytoskeletal reorganization (Fig. 3). In contrast, osteoclast on OPN did not spread in response to M-CSF. This was anticipated as OPN itself induces osteoclast spreading (Fig. 2). On VN, a change in the planar area of cells with 11–20 nuclei was noted; however, those changes were not significant, possibly reflecting the mixed morphologies observed in this group.

EXTRACELLULAR pH OF CULTURES ON FN AND VN ARE LOWER THAN THAT ON OPN

Extracellular pH has previously been shown to affect osteoclast morphology. Nordström et al. [1997] found that lowering the extracellular pH from 7.5 to 7.0 for 24 h increased the proportion of compact osteoclasts from 8 ± 2% to 24.5 ± 6%. In light of these findings, we hypothesized that changes in pH of the cultures on FN, VN, and OPN might be responsible for the morphological differences of osteoclasts formed on these ECM proteins. To test this hypothesis, the extracellular pH of the osteoclast cultures differentiated on these matrix proteins was measured. Coinciding with Nordström's findings, the extracellular pH of osteoclasts on FN, where 25% of the osteoclasts assumed a compact morphology, was 7.24 ± 0.01. On VN, where 12% of the cells were compact, the pH was 7.29 ± 0.02 (Fig. 4). On the contrary, the OPN group, where the highest

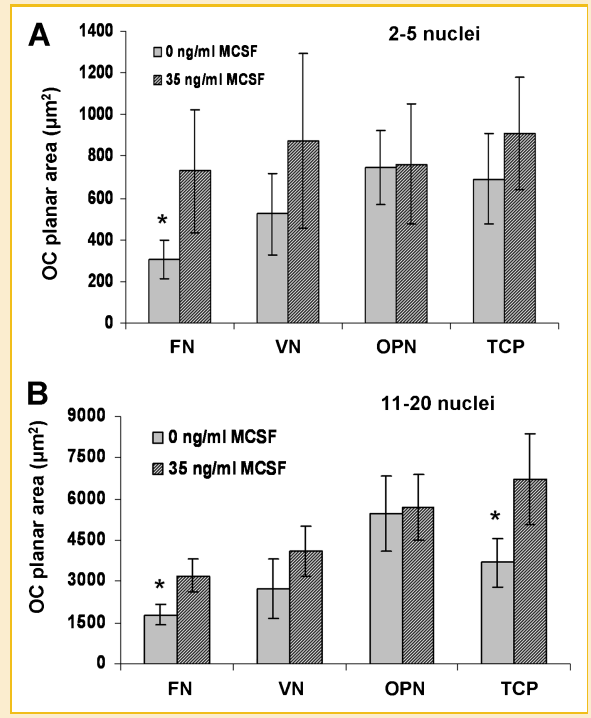

Fig. 3. M-CSF treatment causes osteoclast spreading on FN while osteoclasts on OPN fail to spread. RAW cells were plated on TCP dishes precoated with FN, VN, and OPN at 10 µg/ml. RAW cells were differentiated into osteoclasts for 96 h in the presence of 75 ng/ml RANKL. At 96 h, the cultures were washed 3× with cold PBS–Ca–Mg. The cells were incubated with PBS–Ca–Mg for 45 min at 37°C and 5% CO_2. The cultures were subsequently incubated with media FBS with or without 35 ng/ml M-CSF for 2.5 h. The cultures were fixed and stained for TRAP activity. The perimeter of TRAP+ osteoclasts was outlined manually and the area was measured using Openlab® imaging system. Osteoclasts were divided into groups based on their size determined by the number of nuclei/osteoclast; 2 to 5 nuclei (A) and 11 to 20 nuclei (B). A total of 130 osteoclasts were measured per treatment group. Each data point represents the mean ± SD. Similar results were obtained in three different experiments.

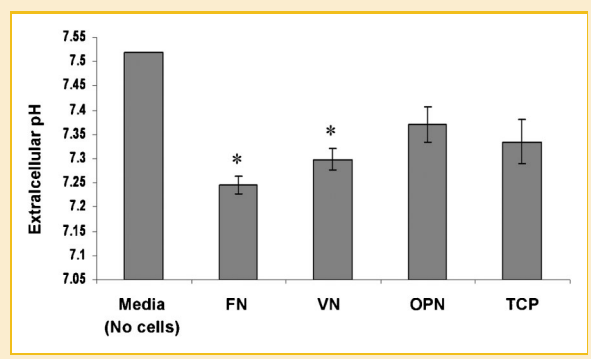

Fig. 4. The effect of ECM proteins on extracellular pH of culture media. RAW cells were plated on TCP dishes precoated with FN, VN, and OPN at 10 µg/ml. RAW cells were differentiated into osteoclasts for 96 h in the presence of 75 ng/ml RANKL. At 96 h, the conditioned media from the cultures was removed and pH determined. Each data point represents the pooled results from four dishes per treatment and is expressed per well (means ± SD). Similar results were obtained in three different experiments.

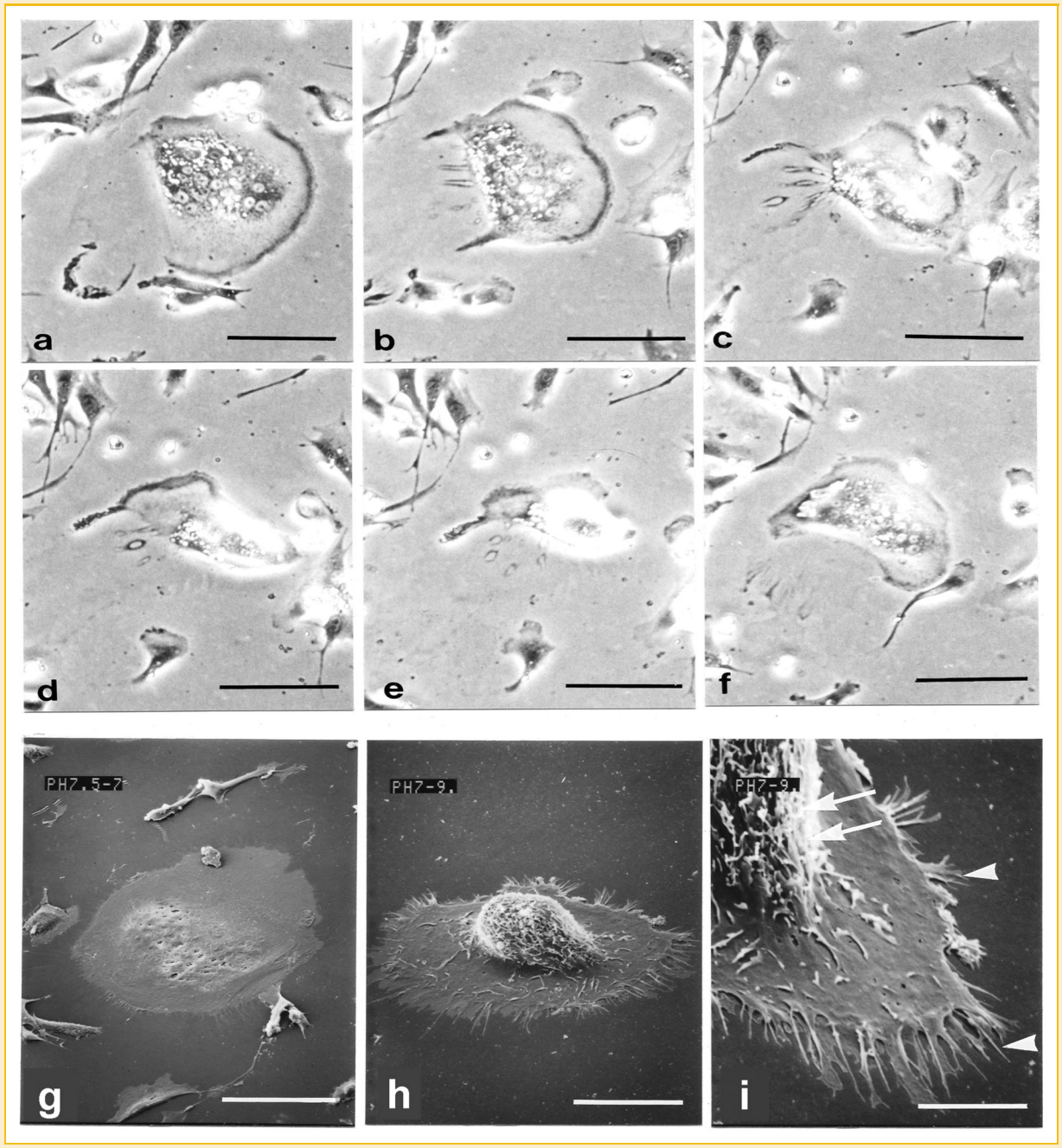

Fig. 5. Phase-contrast and scanning electron micrographs demonstrate the morphological cycling of an osteoclast at pH 7.0. Rabbit osteoclasts were cultured in 35 mm dishes for 16 h before they were washed with bicarbonate-free α-MEM and then incubated with bicarbonate-free HEPES buffered α-MEM of pH 7.0. Phase-contrast images were acquired at the following intervals: (a) time 0, (b) 30 min, (c) 60 min, (d) 75 min, (e) 90 min, (f) 120 min. The osteoclast depicted can be seen altering its morphology from spread (a) to compact (e) and spread again (f). The compact phase was defined as the time during which a complete bright ring of reflected light can be seen. Scale bars are 50 μm. Scanning electron micrographs of osteoclasts cultured as described above show an osteoclast in spread (g) and compact phase (h,i). i: Higher magnification of the periphery of the osteoclast seen in (h). The compact osteoclast in (i) is dome shaped with numerous ruffling on the basolateral surface (arrows) and dense filopodial projections (arrow heads). Scale bars, 60 μm (g); 15 μm (h); 6 μm (i).

percentage of spread osteoclasts was seen (16%), had the highest extracellular pH of 7.37 ± 0.03. Thus the morphological variations observed between different substrates correlate with the changes one would expect as a result of the pH of the respective culture media.

OSTEOCLASTS CYCLE BETWEEN SPREAD AND COMPACT MORPHOLOGIES AND THE RATE OF THESE CHANGES DEPENDS ON OSTEOCLAST SIZE AND EXTRACELLULAR pH

The correlation between extracellular pH and the prevalence of a specific morphology indicates that pH plays an important regulatory

role. Hence, to investigate how pH regulates osteoclast morphology, we used time-lapse microscopy of authentic rabbit osteoclasts. Figure 5 illustrates the morphological cycle of a rabbit osteoclast and outlines how we define the difference between spread and compact osteoclast morphologies in the subsequent figures. Figure 5a–f is a series of phase-contrast micrographs of an osteoclast cultured at pH 7.0. As seen in these images, an osteoclast is continuously undergoing morphological changes between spread (Fig. 5a), compact 90 min later (Fig. 5e), and then spreading again after another 30 min. An osteoclast with its nuclei easily recognizable was considered to be spread. An osteoclast with a rounded basolateral surface reflecting the light, giving it a bright ring appearance and concealing its nuclei, was considered to be compact. Microstructural differences between spread and compact could also be seen using scanning electron microscopy (Fig. 5g–i). Figure 5g shows osteoclasts in the spread phase as flat and with few surface protrusions. In contrast, osteoclasts in compact phase were globular or dome-shaped with more ruffling of the basolateral surface. They also had numerous filopodial projections at their periphery (Fig. 5h,i).

Next, we proceeded to investigate the effect of extracellular pH on the osteoclast morphological cycle; changes in osteoclast area and motility were recorded for 6 h at pH 7.5, after which the media was switched to pH 7.0 for an additional 5–9 h. Because of the differences in spreading between large and small osteoclasts that were previously noted (Fig. 3) the measurements in Figure 6 are also grouped according to osteoclast size (nuclei number/OC). For small osteoclasts, the area descriptor was not affected by lowering the pH to 7.0 yet the motility descriptor increased from 1.11 to 1.34 (Fig. 6A). Small osteoclasts also significantly increased the frequency of morphology cycling at pH 7.0 compared to pH 7.5.

When the results from small osteoclasts were compared to those from large osteoclasts, significant differences in cycling patterns could be seen. Large osteoclasts were found to be predominantly in a spread morphology at pH 7.5 and cycled between spread and large morphologies only when the pH was dropped to 7.0. This was accompanied by an increase in the spread area during the spread phase.

Table I summarizes the average duration small osteoclasts remained in spread and compact phases at pH 7.5 and 7.0. The average compact phase duration for a small osteoclast at pH 7.5 was 25.6 min and the duration of a spread phase was 62.5 min. At pH 7.0, the duration of both phases decreased significantly; small osteoclasts stayed in a compact phase for 14.1 min and in a spread phase for only 15.7 min. Thus the number of cycles per hour of a small osteoclast increased by 3-fold at pH 7.0 compared to that at pH 7.5, and that on average, a small osteoclast stayed compact twice as long at the lower pH (Table I).

We next examined the pH*i* associated with these cycling events of an osteoclast maintained at pH 7.0. As shown in Table II, the average pH*i* of a compact osteoclast was 7.00. The pH*i* of spread osteoclasts on the other hand was 7.34 (Table II).

To determine the mechanisms involved in this pH regulation, the role of the various enzymes involved in osteoclast pH homeostasis were examined. Because of their established role in controlling osteoclast pH*i*, V-ATPase, HCO_3^-/Cl^- exchanger, Na^+/H^+ antiporter, and carbonic anhydrase were evaluated. Specific inhibitors against these enzymes were added at pH 7.0 and the rate of morphological cycling; osteoclast motility and spreading were recorded. The addition of the V-ATPase specific inhibitor bafilomycin A1 increased the duration of the compact phase 4fold while that of the spread phase decreased (Table III). Bafilomycin A1did not affect motility on the basis of time-lapse microscopy. The inhibition of the HCO_3^-/Cl^- exchanger by DIDS and the Na^+/H^+ antiporter by amiloride had the same effect on the duration of the osteoclast compact phase but their effects on the duration of the spread were less pronounced. Finally, inhibiting carbonic anhydrase by acetazolamide had no effect on the length of either phase. Morphological changes caused by these inhibitors were reversible and the cells were able to recover after the inhibitors were washed out indicating that the effects seen were not due to cell toxicity (data not shown).

DISCUSSION

The cycling of an osteoclast through its different morphologies is essential to its optimal function. In this investigation we examined how certain extracellular factors regulate osteoclast shape.

Our data show that differentiating osteoclasts on different ECM differentially regulates morphology. FN resulted in a predominantly compact population, VN primarily migratory, and spread osteoclasts where mostly seen on OPN. These results suggest that the ECM proteins regulate the cytoskeleton via altered signaling mediated through their podosomes. In addition to the variations in osteoclast shape, we noticed differences in osteoclast size as defined by their planar area. Osteoclasts on FN and VN were smaller than on OPN, and this difference was maintained even when planar area was normalized to nuclei number. This difference may reflect enhancement of cell spreading on OPN, compared to the increased cell polarity and compactness on FN and VN. In contrast to our findings, Hu et al. found that mature rat osteoclasts that attached to FN and OPN were larger and contained extended lamellipodia with an average of six to seven nuclei compared to those which adhered on prothrombin and thrombin [Hu et al., 2008]. These contradictory observations may reflect differences in experimental design and cell type. In their study, mature primary rat osteoclasts were plated onto these matrix proteins while a mouse cell line was used in this study and the cells were differentiated into osteoclasts in the presence of the ECM proteins.

To ask whether the different morphologies reflect a defect in the activation of osteoclast spreading, the cells' ability to respond to M-CSF was assessed. M-CSF induces osteoclast spreading and cytoskeletal reorganization on glass and plastic, and resorption on mineralized substrates [Pilkington et al., 1998; Teti et al., 1998; Lees and Heersche, 1999; Nakamura et al., 1999; Gramoun et al., 2007]. The cytokine's action is mediated via phosphatidylinositol 3-kinase (PI3-kinase) which in turn induces integrin αvβ3 activation via the non-receptor tyrosine kinase c-src [Nakamura et al., 2003]. To determine any defects in the M-CSF-αvβ3-actin cytoskeleton axis, we challenged osteoclasts by inducing retraction followed by M-CSF to provoke cell spreading. Osteoclasts on FN and VN spread

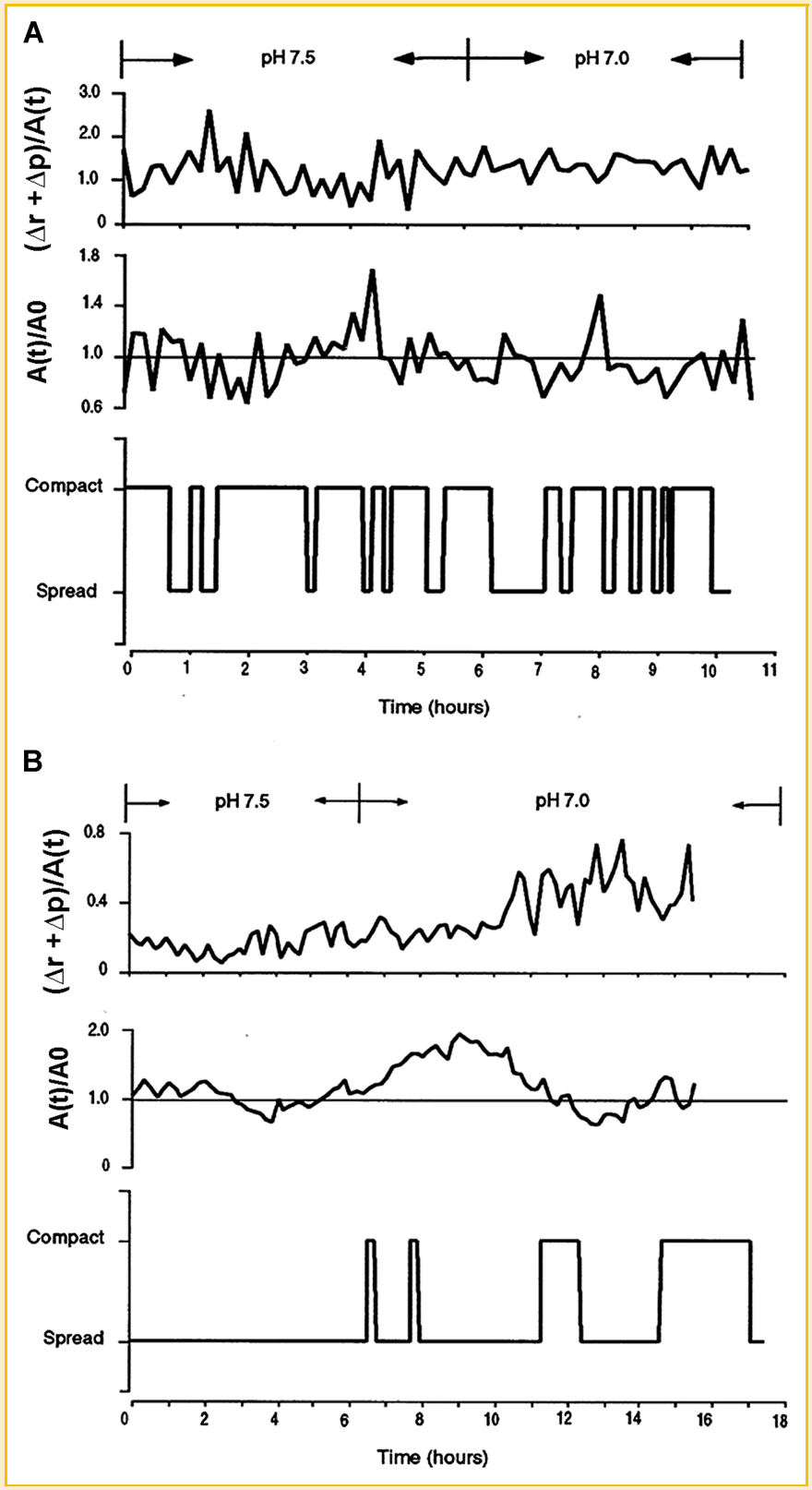

Fig. 6. Time course of morphological cycling of small and large osteoclasts at pH 7.5 and pH 7.0. Rabbit osteoclasts were cultured in 35 mm dishes for 16 h before they were washed with bicarbonate-free α-MEM and then incubated with bicarbonate-free HEPES buffered α-MEM pH 7.5 for 6 h. This was followed a media change where the osteoclasts were cultured for an additional 5–9 h at pH 7.0. Phase-contrast images were acquired at equal time intervals and the following parameters were calculated: A(t)/A0 denoting cell spreading area, and ([ΔP] + [Δr])/A(t) denoting cell motility. A: Time course of a small osteoclast (maximum diameter = 50 μm, number of nuclei = 5), (b) time course of a large osteoclast (maximum diameter = 150 μm, number of nuclei = 28).

TABLE I. The Duration of the Compact and Spread Phases of Small Osteoclasts at pH 7.0 and 7.5

	Compact (A) (min)	Spread (B) (min)	(A/B)	{60/(A + B)}
pH 7.5	25.6 ± 6.57	62.5 ± 14.16	0.41	0.68
pH 7.0	14.1 ± 1.49	15.7 ± 1.95	0.9	2.01

The average duration in min of compact and spread phases of osteoclasts, expressed as mean ± SEM. The ratio of compact to spread phase in time (A/B) and the number of cycles per hour {60/(A + B)}; n = 15 in each group.

appropriately in response to M-CSF demonstrating that their smaller size was not due to improper cytoskeletal reorganization. In contrast, osteoclasts on OPN did not spread in response to M-CSF. This might be due to the fact that morphological changes of osteoclasts on OPN are independent of the M-CSF signaling pathway. Teti et al. [1998] performed similar experiments on mature rabbit osteoclasts and found that osteoclasts on OPN did spread in response to M-CSF, however it is not clear from their figure whether the changes in area were significant or not.

Experiments by Nordström et al., showing that osteoclast morphology is affected by extracellular pH suggested a mechanism by which chronic metabolic acidosis leads to bone loss. When they mimicked acidosis by lowering extracellular pH to 6.5, a 15% increase in cells with a compact phenotype occurred [Nordström et al., 1997]. This result is similar to the increase in the percentage of compact osteoclasts we saw on FN. Consistent with their findings; when the extracellular pH in our cultures was measured, the pH on FN was substantially lower than on OPN suggesting that each matrix protein differentially affects the extracellular pH.

Further examination revealed that morphological cycling of osteoclasts is affected by extracellular pH. Both osteoclast motility and the frequency of the morphological cycle were increased at pH 7.0 compared to pH 7.5, resulting in an increase in the total duration of an osteoclast in a compact phase. This could explain the increase in the percentage of compact osteoclasts at low pH [Nordström et al., 1997] and on FN seen in Figure 2A. This also shows that compact osteoclasts on TCP have a similar behavior to polarized osteoclasts on bone. These findings are also compatible with those showing an increase in osteoclast polarity and resorption at a low pH [Arnett and Dempster, 1986; Shibutani and Heersche, 1993; Arnett et al., 1994; Nordström et al., 1997].

Another similarity between compact osteoclasts on TCP and bone lies in the regulation of their cytoplasmic pH. Actively resorbing osteoclasts dissolve mineralized tissue by pumping H^+ into the resorption lacunae. To do so, polarized non-resorbing osteoclasts accumulate protons prior to proton extrusion. Similarly, we found that compact osteoclasts on TCP have a lower pH*i* than in the spread phase. The process of cytosolic proton accumulation involves V-ATPases, HCO_3^-/Cl^- exchangers, Na^+/H^+ antiporters, and carbonic anhydrase II. We used specific inhibitors to each of these enzymes to assess their contribution to the regulation of pH*i* and osteoclast morphology. The duration of the compact phase increased when inhibiting the V-ATPase, the HCO_3^-/Cl^- exchanger or the Na^+/H^+ antiporter. The frequency of the morphological cycle on the other hand decreased. In contrast, carbonic anhydrase II had no effect, either because of a suboptimal concentration of acetazolamide [Hunter et al., 1991] or alternatively that a different mechanism of proton production exists. In summary, we show that extracellular pH and osteoclast shape can be determining factors of pH regulation.

The link between pH*i* and FN has been established in studies investigating the role of the ECM proteins in cell proliferation. The rate of cell proliferation was found to be affected by pH*i*, which in turn, was dependent on cell spreading. Schwartz et al. [1989] showed that conditions that induced fibroblast spreading increased cell proliferation, and that was also accompanied by an increase in pH*i*. Similar effects on pH*i* were found when capillary endothelial cells were cultured on FN [Ingber et al., 1990]. Subsequently, they were able to demonstrate that FN led to $\alpha5\beta1$ clustering, which activated the Na^+/H^+ anti-porter, in turn driving protons out of the cells and raising pH*i* [Schwartz et al., 1991]. Based on these findings, we propose the following model for how FN causes osteoclast activation and compact morphology. This model is based on the fact that RAW cell cultures contain two cell populations. At 48 h, the majority of cells are undifferentiated and TRAP + mononuclear cells. By 72 h, a second population of multinucleated osteoclasts starts to appear. On FN, we found that the mononuclear cells were significantly more spread than on TCP. Similar to Schwartz et al. observations with fibroblast, we propose that the spreading of the mononuclear cells is accompanied by activation of the Na^+/H^+ antiporter, an elevation of their pH*i* and acidification of their extracellular milieu. The extracellular acidification would then activate osteoclasts and result in a more compact morphology.

TABLE II. Intracellular pH in Compact and Spread Osteoclasts

	Intracellular pH
Compact phase	7.00 ± 0.15
Spread phase	7.34 ± 0.14

Cells were cultured in medium at pH 7.0 for 3 h before their intracellular pH was measured. Results are expressed as mean ± SD, where n = 20 in each group.

TABLE III. The Effects of Bafilomycin A1(BFA), Acetazolamide (AZ), DIDS, and Amiloride (Am) on the Duration of Compact and Spread Phases of Osteoclasts

	Compact (min)	Spread (min)	Cell size[a] (μm)
Control	13.0 ± 2.1	25.7 ± 8.1	79.2
BAF (100 nM)	58.5 ± 13.5*	17. 6 ± 6.7	n = 7
Control	26.4 ± 5.5	22.7 ± 8.9	85
Am (1 mM)	139.9 ± 24.7*	42.2 ±28.6	n = 7
Control	19.8 ± 4.1	26.0 ± 8.4	88.7
DIDS (100 μM)	88.4 ± 21.5*	21.4 ± 4.0	n = 8
Control	10.1 ± 1.9	22.5 ± 3.7	112.5
AZ (10 μM)	18.7 ± 5.8	13.6 ± 3.4	n = 5

Results are the mean ± SEM of each duration.
[a]Cell size is represented as the average of maximum osteoclast diameter measured, where n = number of osteoclasts measured.
*$P < 0.05$ compared to the control.

One of the intriguing aspects of osteoclasts physiology is their heterogeneous behavior based on their size. Large osteoclasts ($\geq$10 nuclei) are significantly different in their behavior and resorptive activity from small osteoclasts (2–5 nuclei) [Piper et al., 1992]. Large osteoclasts are hyperactive, produce more pits [Lees and Heersche, 1999; Lees et al., 2001], and are more often actively resorbing [Lees et al., 2001]. Large osteoclasts are also found predominantly in pathological bone loss conditions and sites of bone inflammation [Makris and Saffar, 1982; Kaye et al., 1985; Singer, 1996]. Additionally, large osteoclasts have a higher pH*i* [Lees and Heersche, 2000] and a higher expression of V-ATPases responsible for this pH regulation [Manolson et al., 2003]. In contrast, small osteoclasts have a lower pH*i* regulated by V-ATPases and Na^+/H^+ antiporters [Lees and Heersche, 2000]. More recently it was shown that large and small osteoclasts also differentially express several receptors and osteoclast phenotypic markers that activate different signaling pathways [Trebec et al., 2007].

In line with these differences between those two osteoclast populations, we also found that large and small osteoclasts differ in their behavior on ECM proteins. Small osteoclasts on FN showed a greater spreading response than large osteoclasts in response to M-CSF treatment. Furthermore, large and small osteoclasts exhibited different cycling patterns. At a physiologic pH, small osteoclasts spontaneously cycled between spread and compact morphologies approximately twice per hour while large osteoclasts showed no morphological changes. Upon extracellular acidification, small osteoclasts cycled 4–5 times per hour and the large osteoclasts cycled ~0.5 times per hour.

The interaction between osteoclasts and FN, VN, and OPN is mainly RGD dependent. However, these interactions differentially regulate osteoclast morphology indicating that several integrins and surface receptors are involved. In osteoclasts, the integrin $\alpha v\beta 3$ is the most abundant integrin; however, other integrins are also expressed [Nesbitt et al., 1993]. In a simultaneous study [Gramoun et al., in preparation] we have shown that osteoclasts formed on FN have a higher expression of the integrin $\alpha v\beta 3$ compared to VN, OPN, and the TCP control. Additionally, the integrin $\alpha 5\beta 1$ was present on osteoclasts differentiated on FN and its level was higher than those seen on TCP. We found that $\alpha v\beta 3$ inhibited osteoclastogenesis, while $\alpha 5\beta 1$ was responsible for mediating osteoclast attachment on FN. We hypothesize that the differential expression of $\alpha v\beta 3$ and $\alpha 5\beta 1$ and other surface receptors such as CD44 are in part responsible for the reported effects of osteoclasts morphology on ECM proteins. Downstream of $\alpha v\beta 3$ and $\alpha 5\beta 1$ activation, signaling pathways could be increasing the pH*i*, in turn dropping the extracellular pH which also affects the morphological cycle of osteoclasts.

Finally, it was shown that extracellular acidosis increases osteoclast polarization and resorption [Carano et al., 1993; Shibutani and Heersche, 1993] via increasing the H^+-pumping activity of the V-ATPase [Nordström et al., 1997]. This is compatible with our findings that low extracellular pH increased the percentage of osteoclasts in a compact phase and the total time an osteoclast spends in that phase. Taken together, these data suggest that compact osteoclasts on TCP have structural and functional similarities with their polarized counterparts on mineralized surfaces.

In summary, we have identified ECM proteins and pH as co-players involved in regulating osteoclast shape and present data indicating that they connected. Our data suggests that in addition to the canonical mechanism controlling osteoclast skeletal organization triggered by the mineral content of a matrix, ECM proteins and extracellular acidification should be considered as contributing factors modulating this process.

REFERENCES

Akisaka T, Yoshida H, Inoue S, Shimizu K. 2001. Organization of cytoskeletal F-actin, G-actin, and gelsolin in the adhesion structures in cultured osteoclast. J Bone Miner Res 16:1248–1255.

Arkett SA, Dixon SJ, Sims SM. 1992. Substrate influences rat osteoclast morphology and expression of potassium conductances. J Physiol 458:633–653.

Arnett TR, Dempster DW. 1986. Effect of pH on bone resorption by rat osteoclasts in vitro. Endocrinology 119:119–124.

Arnett TR, Boyde A, Jones SJ, Taylor ML. 1994. Effects of medium acidification by alteration of carbon dioxide or bicarbonate concentrations on the resorptive activity of rat osteoclasts. J Bone Miner Res 9:375–379.

Asotra S, Gupta AK, Sodek J, Aubin JE, Heersche JN. 1994. Carbonic anhydrase II mRNA expression in individual osteoclasts under ''resorbing'' and ''nonresorbing'' conditions. J Bone Miner Res 9:1115–1122.

Badowski C, Pawlak G, Grichine A, Chabadel A, Oddou C, Jurdic P, Pfaff M, Albiges-Rizo C, Block MR. 2008. Paxillin phosphorylation controls invadopodia/podosomes spatiotemporal organization. Mol Biol Cell 19:633–645.

Bastani B, Ross FP, Kopito RR, Gluck SL. 1996. Immunocytochemical localization of vacuolar H+-ATPase and $Cl^-HCO_3^{--}$ anion exchanger (erythrocyte band-3 protein) in avian osteoclasts: Effect of calcium-deficient diet on polar expression of the H+-ATPase pump. Calcif Tissue Int 58:332–336.

Carano A, Schlesinger PH, Athanasou NA, Teitelbaum SL, Blair HC. 1993. Acid and base effects on avian osteoclast activity. Am J Physiol 264:C694–C701.

Chellaiah MA, Hruska KA. 2003. The integrin alpha(v)beta(3) and CD44 regulate the actions of osteopontin on osteoclast motility. Calcif Tissue Int 72:197–205.

Desai B, Ma T, Chellaiah MA. 2008. Invadopodia and matrix degradation, a new property of prostate cancer cells during migration and invasion. J Biol Chem 283:13856–13866.

Edwards JC, Cohen C, Xu W, Schlesinger PH. 2006. c-Src control of chloride channel support for osteoclast HCl transport and bone resorption. J Biol Chem 281:28011–28022.

Flores ME, Norgard M, Heinegard D, Reinholt FP, Andersson G. 1992. RGD-directed attachment of isolated rat osteoclasts to osteopontin, bone sialoprotein, and fibronectin. Exp Cell Res 201:526–530.

Geblinger D, Geiger B, Addadi L. 2009. Surface-induced regulation of podosome organization and dynamics in cultured osteoclasts. Chembiochem 10:158–165.

Gramoun A, Shorey S, Bashutski JD, Dixon SJ, Sims SM, Heersche JN, Manolson MF. 2007. Effects of Vitaxin, a novel therapeutic in trial for metastatic bone tumors, on osteoclast functions in vitro. J Cell Biochem 102:341–352.

Gramoun A, Azizi N, Sodek J, Heersche JNM, Nakchbandi I, Manolson MF. 2010. The extracellular matrix protein fibronectin enhances osteoclast activity via nitric oxide and interleukin-1β mediated signalling pathways. In preparation.

Gupta A, Edwards JC, Hruska KA. 1996. Cellular distribution and regulation of NHE-1 isoform of the NA-H exchanger in the avian osteoclast. Bone 18:87–95.

Hall TJ, Chambers TJ. 1990. Na+/H+ antiporter is the primary proton transport system used by osteoclasts during bone resorption. J Cell Physiol 142:420–424.

Hu Y, Ek-Rylander B, Karlstrom E, Wendel M, Andersson G. 2008. Osteoclast size heterogeneity in rat long bones is associated with differences in adhesive ligand specificity. Exp Cell Res 314:638–650.

Hunter SJ, Rosen CJ, Gay CV. 1991. In vitro resorptive activity of isolated chick osteoclasts: Effects of carbonic anhydrase inhibition. J Bone Miner Res 6:61–66.

Ingber DE, Prusty D, Frangioni JV, Cragoe EJ, Jr., Lechene C, Schwartz MA. 1990. Control of intracellular pH and growth by fibronectin in capillary endothelial cells. J Cell Biol 110:1803–1811.

Jurdic P, Saltel F, Chabadel A, Destaing O. 2006. Podosome and sealing zone: Specificity of the osteoclast model. Eur J Cell Biol 85:195–202.

Kanehisa J, Heersche JN. 1988. Osteoclastic bone resorption: In vitro analysis of the rate of resorption and migration of individual osteoclasts. Bone 9: 73–79.

Kaye M, Zucker SW, Leclerc YG, Prichard S, Hodsman AB, Barre PE. 1985. Osteoclast enlargement in endstage renal disease. Kidney Int 27:574–581.

Kornak U, Kasper D, Bosl MR, Kaiser E, Schweizer M, Schulz A, Friedrich W, Delling G, Jentsch TJ. 2001. Loss of the ClC-7 chloride channel leads to osteopetrosis in mice and man. Cell 104:205–215.

Lakkakorpi PT, Vaananen HK. 1991. Kinetics of the osteoclast cytoskeleton during the resorption cycle in vitro. J Bone Miner Res 6:817–826.

Lees RL, Heersche JN. 1999. Macrophage colony stimulating factor increases bone resorption in dispersed osteoclast cultures by increasing osteoclast size. J Bone Miner Res 14:937–945.

Lees RL, Heersche JN. 2000. Differences in regulation of pH(i) in large ($\geq$10 nuclei) and small ($\leq$5 nuclei) osteoclasts. Am J Physiol Cell Physiol 279: C751–C761.

Lees RL, Sabharwal VK, Heersche JN. 2001. Resorptive state and cell size influence intracellular pH regulation in rabbit osteoclasts cultured on collagen-hydroxyapatite films. Bone 28:187–194.

Luxenburg C, Geblinger D, Klein E, Anderson K, Hanein D, Geiger B, Addadi L. 2007. The architecture of the adhesive apparatus of cultured osteoclasts: From podosome formation to sealing zone assembly. PLoS ONE 2:e179.

Makris GP, Saffar JL. 1982. Quantitative relationship between osteoclasts, osteoclast nuclei and the extent of the resorbing surface in hamster periodontal disease. Arch Oral Biol 27:965–969.

Manolson MF, Yu H, Chen W, Yao Y, Li K, Lees RL, Heersche JN. 2003. The a3 isoform of the 100-kDa V-ATPase subunit is highly but differentially expressed in large ($\geq$10 nuclei) and small ($\leq$5 nuclei) osteoclasts. J Biol Chem 278:49271–49278.

Nakamura I, Pilkington MF, Lakkakorpi PT, Lipfert L, Sims SM, Dixon SJ, Rodan GA, Duong LT. 1999. Role of alpha(v)beta(3) integrin in osteoclast migration and formation of the sealing zone. J Cell Sci 112(Pt 22): 3985–3993.

Nakamura I, Rodan GA, Duong le T. 2003. Distinct roles of p130Cas and c-Cbl in adhesion-induced or macrophage colony-stimulating factor-mediated signaling pathways in prefusion osteoclasts. Endocrinology 144:4739–4741.

Nesbitt S, Nesbit A, Helfrich M, Horton M. 1993. Biochemical characterization of human osteoclast integrins. Osteoclasts express alpha v beta 3, alpha 2 beta 1, and alpha v beta 1 integrins. J Biol Chem 268:16737–16745.

Nordström T, Rotstein OD, Romanek R, Asotra S, Heersche JN, Manolson MF, Brisseau GF, Grinstein S. 1995. Regulation of cytoplasmic pH in osteoclasts. Contribution of proton pumps and a proton-selective conductance. J Biol Chem 270:2203–2212.

Nordström T, Shrode LD, Rotstein OD, Romanek R, Goto T, Heersche JN, Manolson MF, Brisseau GF, Grinstein S. 1997. Chronic extracellular acidosis induces plasmalemmal vacuolar type H+ ATPase activity in osteoclasts. J Biol Chem 272:6354–6360.

Owens J, Chambers TJ. 1993. Macrophage colony-stimulating factor (M-CSF) induces migration in osteoclasts in vitro. Biochem Biophys Res Commun 195:1401–1407.

Pilkington MF, Sims SM, Dixon SJ. 1998. Wortmannin inhibits spreading and chemotaxis of rat osteoclasts in vitro. J Bone Miner Res 13:688–694.

Pilkington MF, Sims SM, Dixon SJ. 2001. Transforming growth factor-beta induces osteoclast ruffling and chemotaxis: Potential role in osteoclast recruitment. J Bone Miner Res 16:1237–1247.

Piper K, Boyde A, Jones SJ. 1992. The relationship between the number of nuclei of an osteoclast and its resorptive capability in vitro. Anat Embryol (Berl) 186:291–299.

Saltel F, Destaing O, Bard F, Eichert D, Jurdic P. 2004. Apatite-mediated actin dynamics in resorbing osteoclasts. Mol Biol Cell 15:5231–5241.

Schlesinger PH, Blair HC, Teitelbaum SL, Edwards JC. 1997. Characterization of the osteoclast ruffled border chloride channel and its role in bone resorption. J Biol Chem 272:18636–18643.

Schwartz MA, Both G, Lechene C. 1989. Effect of cell spreading on cytoplasmic pH in normal and transformed fibroblasts. Proc Natl Acad Sci USA 86:4525–4529.

Schwartz MA, Lechene C, Ingber DE. 1991. Insoluble fibronectin activates the Na/H antiporter by clustering and immobilizing integrin alpha 5 beta 1, independent of cell shape. Proc Natl Acad Sci USA 88:7849–7853.

Shibutani T, Heersche JN. 1993. Effect of medium pH on osteoclast activity and osteoclast formation in cultures of dispersed rabbit osteoclasts. J Bone Miner Res 8:331–336.

Singer FR. 1996. Paget's disease of bone possible viral basis. Trends Endocrinol Metab 7:258–261.

Teti A, Taranta A, Migliaccio S, Degiorgi A, Santandrea E, Villanova I, Faraggiana T, Chellaiah M, Hruska KA. 1998. Colony stimulating factor-1-induced osteoclast spreading depends on substrate and requires the vitronectin receptor and the c-src proto-oncogene. J Bone Miner Res 13:50–58.

Thomas JA, Buchsbaum RN, Zimniak A, Racker E. 1979. Intracellular pH measurements in Ehrlich ascites tumor cells utilizing spectroscopic probes generated in situ. Biochemistry 18:2210–2218.

Trebec DP, Chandra D, Gramoun A, Li K, Heersche JN, Manolson MF. 2007. Increased expression of activating factors in large osteoclasts could explain their excessive activity in osteolytic diseases. J Cell Biochem 101:205–220.

Zaidi M, Alam AS, Shankar VS, Bax BE, Moonga BS, Bevis PJ, Pazianas M, Huang CL. 1992. A quantitative description of components of in vitro morphometric change in the rat osteoclast model: Relationships with cellular function. Eur Biophys J 21:349–355.